A 75-110 GHz Digitally-Probed Artificial Dielectric Phase Demodulator in 65nm CMOS

A. Tang, G. Virbila, T. LaRocca, and M.F. Chang
University of California, Los Angeles, California.

***Abstract*—This paper introduces the Digitally Probed Artificial Dielectric (DiPAD) demodulator: a direct carrier frequency and phase demodulator that operates by digitally detecting the voltage standing-wave response of periodically loaded transmission lines with CMOS sensors. The proposed demodulator allows for the direct demodulation of phase or frequency encoded signals without the need for an analog to digital converter, enabling the construction of a simpler, more power efficient mm-wave receiver. The proposed DiPAD demodulator was implemented in 65nm CMOS technology and operates at carrier frequencies up to 110 GHz, while consuming only 0.47mW of DC power and occupying only 0.16mm^2 of silicon area.**

I. INTRODUCTION

Advanced wireless mm-wave communication systems commonly employ digital phase modulation schemes to achieve higher bandwidth efficiency, improved robustness to channel imperfections, and easier digital demodulation. To perform phase-based carrier modulation, mm-wave transmitter systems typically employ digital-to-analog converters (DAC) to translate the outgoing digital data into a modulated analog signal, which is then up-converted by a mixer chain to mm-wave frequencies. While this approach is straight-forward, the high resolution, linearity, and power required by the data converter limits transmitter efficiency and increases design complexity. A similar situation exists in mm-wave receiver systems where the mm-wave carrier is down-converted by a mixer chain and translated back to incoming bits by an analog-to-digital converter (ADC). Again this increases the power consumption and complexity of a mm-wave receiver system. To overcome these limitations, [1] presents a "Digitally Controlled Artificial Dielectric" (DiCAD) element that can directly modulate a mm-wave carrier from the outgoing digital data, without the need for a DAC or up-converting mixer chain. By removing the DAC and mixer chain from the transmitter system, complexity and power consumption are greatly reduced. In response to the unique technique of DiCAD modulation, this paper proposes the digitally-probed artificial dielectric, (DiPAD) which performs the reverse operation of its DiCAD counterpart, directly impressing the mm-wave carrier's phase onto a digital signal for the purposes of frequency or phase demodulation. The proposed DiPAD demodulator achieves the parallel function of the DiCAD in the transmitter by removing the need for an ADC and down-conversion mixer chain in a mm-wave receiver system, again reducing power consumption and receiver complexity.

II. ARTIFICIAL DIELECTRIC

An artificial dielectric is a floating metallic structure that when embedded orthogonally below a coplanar strip transmission line, artificially increases the effective dielectric constant. The DiCAD presented in [1],[2] acts as a permittivity programmable transmission line by alternating the dielectric elements between short and open conditions with a CMOS switch. The major advantage of the artificial dielectric is that the control switch does not lie in the signal path, minimizing insertion loss along the transmission line. The structure of the proposed DiPAD demodulator is almost identical; however, instead of CMOS switches, the DiPAD has small CMOS power sensors or probes placed at each artificial dielectric to measure the signal amplitude at each point along the line. Fig.1 compares the physical construction of both the DiCAD and DiPAD structures.

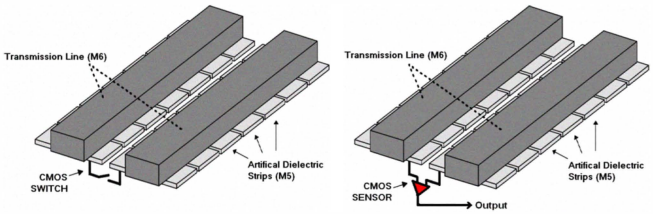

(a) DiCAD Structure (b) DiPAD Structure

Fig. 1. CMOS DiCAD and DiPAD implementations.

III. DIPAD CONFIGURATIONS

The DiPAD can be configured as both a frequency and phase detector depending on the termination conditions placed at each end of the transmission line structure. By placing an input signal at one end of the transmission line and placing a short or open termination condition at the other, the DiPAD can be configured as a frequency detector since the location of the resultant standing-wave null is determined only by the carrier frequency. Alternatively the DiPAD can be configured with input signals at both end, in which case the standing-wave null will be related to the phase difference between the two input sources. The frequency or phase resolution is simply dependent on the number of sensors placed along the DiPAD structure. To demodulate an n-PSK signal a total number of n-1 sensors are be required at equal intervals along a half-wave transmission line. For example in a QPSK operation a total of 3 sensors are needed along 0.5 wavelengths of transmission

978-1-61284-757-3/11/$26.00 C2011 IEEE

line to perform the demodulation. Fig.2a shows the frequency detector configuration of the DiPAD while Fig.2b shows the phase detector configuration.

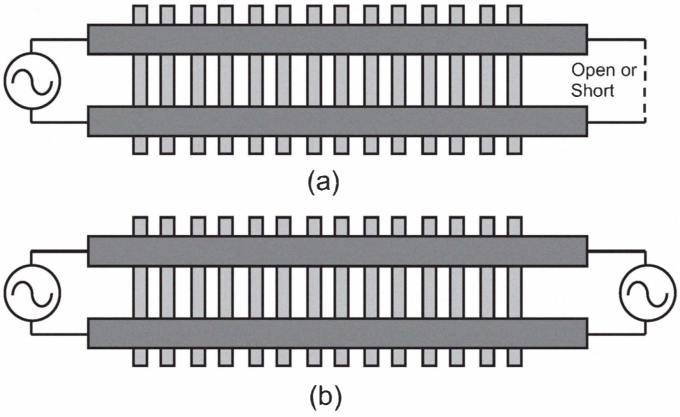

Fig. 2. DiPAD configurations (a) Frequency detector configuration with open or short termination. (b) Phase detector with dual inputs.

IV. DiPAD Voltage Sensor

The DiPAD demodulator operates by first detecting the position of the voltage standing-wave nulls on a transmission line, then converting this position directly into a digital signal representing the detected frequency of phase. To accomplish this the DiPAD contains CMOS sensors placed at each artificial dielectric element which capacitively measure the voltage amplitude at various points along the transmission line.

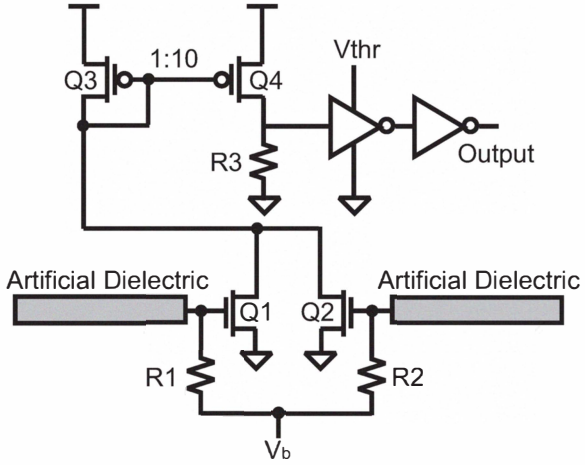

Fig. 3. Schematic diagram of DiPAD digital sensor.

The schematic of the CMOS sensor is shown in Fig.3. CMOS transistors Q1 and Q2 are biased by resistors R1 and R2, and rectify the signal collected by the artificial dielectric strips under the transmission line. The rectified current is amplified by the current mirror composed of Q3 and Q4 with load resistor R3. The output voltage of the amplifier is then applied to a comparator implemented as a cascade of digital CMOS inverters. To provide for fine adjustment of the comparator threshold the first stage of the inverter cascade has an adjustable supply voltage (V_{thr}). The total voltage gain of the sensor from the artificial dielectric strip to the input of the digital inverter will be,

$$A_s = -10\frac{g_{m12}R_3}{\sqrt{2}}$$

,

Where g_{m12} is the trans-conductance of transistors Q1 and Q2, the factor of 10 is the gain of the current mirror formed by Q3 and Q4, and the factor of $\sqrt{2}$ arises from the rectification action of the sensor itself. Since the threshold of the digital inverter will be approximately half of V_{thr} the sensitivity of the sensor can be computed as,

$$S = \frac{1}{10}\frac{V_{thr}}{g_{m12}R_3\sqrt{2}}$$

Note that the sensor output is "1" when the input power is below threshold and the output is "0" when the input power is above threshold. This means that sensors located at a voltage null will produce a "1" while sensors located at positions with voltage will produce a "0".

V. DiPAD Frequency Demodulator

In order to use the DiPAD as a frequency demodulator, a short-circuit termination is placed at one end of the structure while the signal to be demodulated is injected from the other. In this short circuited termination condition the first null of the resultant voltage standing-wave will occur at exactly 0.5 wavelengths from the end of the transmission line. The CMOS sensors connected to the artificial dielectric will return a digital pattern indicating where the 0.5 wavelength null lies along the transmission line.

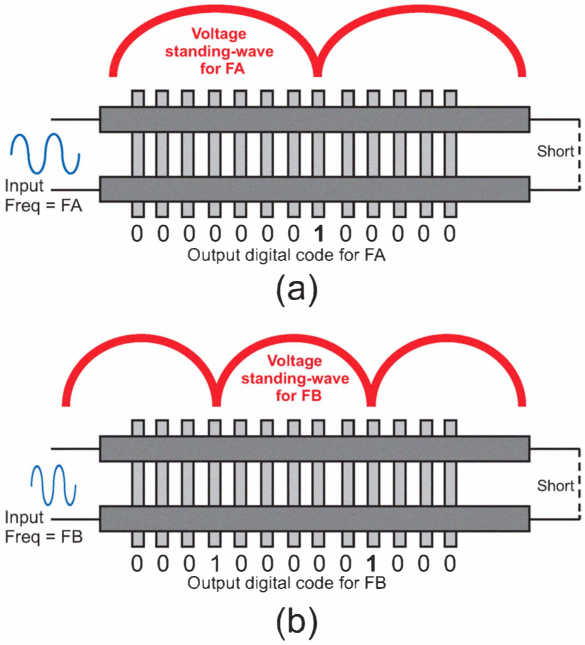

Fig. 4. (a) Voltage standing-wave and digital outputs of DiPAD for input frequency F_A. (b) Voltage standing-wave and digital outputs of DiPAD for input frequency F_B ($F_B > F_A$).

Fig.4a shows the voltage standing-wave and resultant sensor outputs of the DiPAD for carrier frequency F_A. At frequency

978-1-61284-757-3/11/$26.00 C2011 IEEE

F_A the null of the voltage standing-wave lands on the 6th strip from the short termination causing that sensor to return a "1" . This "1" indicates the carrier frequency. In Fig.4b, the DiPAD is excited with a higher frequency F_B, ($F_B > F_A$). At frequency F_B the closest standing-wave null to the short termination lands on the fourth strip producing a "1" at that sensor. This position indicates that frequency F_A is less than F_B since the first "1" lies further from the short termination. In general the right most "1" output from the DiPAD indicates the received carrier frequency. To demodulate FSK signaling, the DiPAD should be designed so that the sensors are placed at the expected voltage null point for each FSK symbol. The frequency resolution of the DiPAD is limited only by the spacing and number of artificial dielectric sensors placed along the transmission line.

VI. DiPAD Phase Demodulator

To configure the DiPAD as a phase demodulator (phase detector) a 0.5 wavelength line at the demodulated frequency is required. The reference phase signal is connected to one end while the signal to be phase demodulated is injected from the other. In this dual input condition the null of the resultant voltage standing wave will depend completely on the length of the line and the relative input phases. The CMOS sensors connected to the artificial dielectric will return a digital pattern indicating where the null lies along the transmission line.

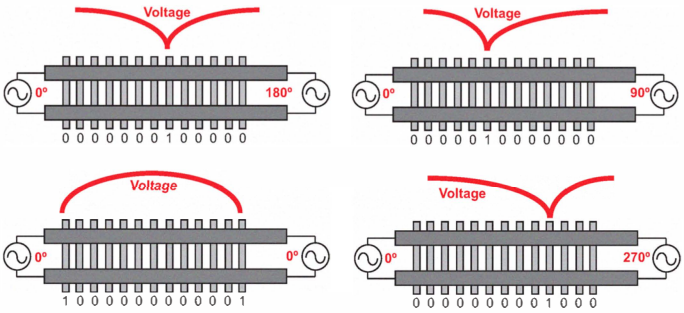

Fig. 5. Voltage standing wave and digital sensor output of DiPAD in phase demodulator configuration with 0, 90, 180, and 270 degree phases.

Fig.5 shows the voltage standing wave and resultant sensor outputs for four different phases commonly used in QPSK signaling. The resulting location of the digital 1 indicates the phase difference between the reference signal and input signal. To demodulate PSK signaling, the DiPAD should again be designed so that the sensors are placed at the expected voltage null point for each PSK symbol. The phase resolution, much like the frequency resolution, is limited only by the spacing and number of artificial dielectric sensors placed along the transmission line.

VII. DiPAD Measurement Results

The proposed DiPAD phase/frequency demodulator was implemented in a 6-metal 1-poly 65nm RF CMOS process. The die photo of the DiPAD structure is shown in Fig.6, with inputs and outputs identified in the layout diagram below the photo. The RF inputs are coupled with a pair of on-chip baluns in order to couple with the single-ended RF probes, and to improve the even mode suppression of the carrier signals injected into the DiPAD. Sensor outputs, DC biasing, supply voltages, and returns are all carried on a single DC 8-pin wedge.

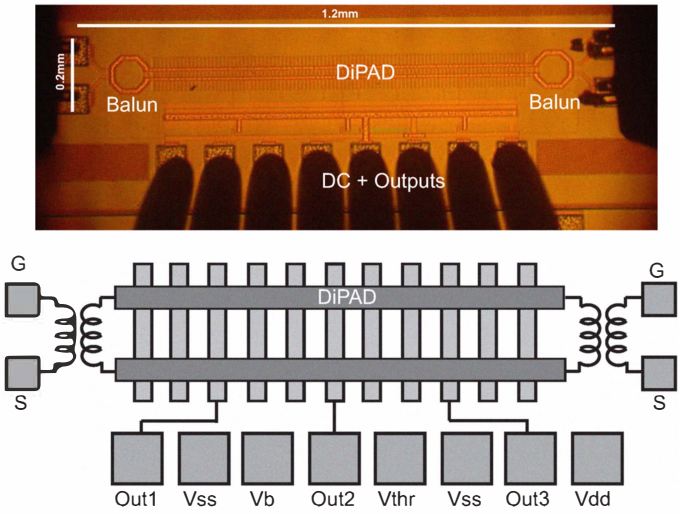

Fig. 6. Die photo and layout diagram of the proposed DiPAD demodulator showing inputs and outputs.

The prototype DiPAD is composed of an 800um section of coplanar transmission line with three equally spaced sensors located on artificial dielectric elements underneath. The transmission line was constructed on the top metal layer and the artificial dielectric strips were constructed on the layer immediately below.

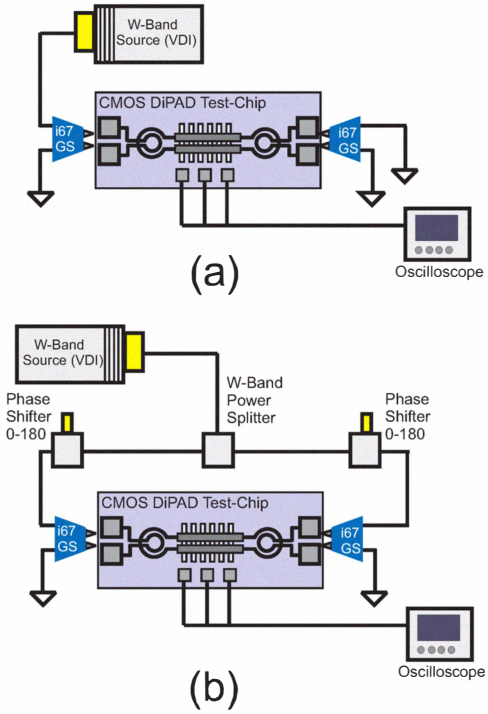

Fig. 7. (a) Measurement setup for frequency demodulation. (b) Measurement setup for phase demodulation.

To test the frequency demodulation performance of the DiPAD, a short termination was placed at one end using a

978-1-61284-757-3/11/$26.00 C2011 IEEE

GS probe, while a continuous-wave (CW) mm-wave signal of 3 dBm power was injected at the other with an SG probe as shown in Fig.7a. The frequency of the injected carrier was swept across the W-band frequency range (75 to 110 GHz) and the sensor response was plotted in Fig.8. As expected the sensor placed furthest away from the short termination (sensor 1) produced a "1" for the lower end of the frequency band, while the sensor closest to the termination (sensor 3) responded at the higher end of the frequency band.

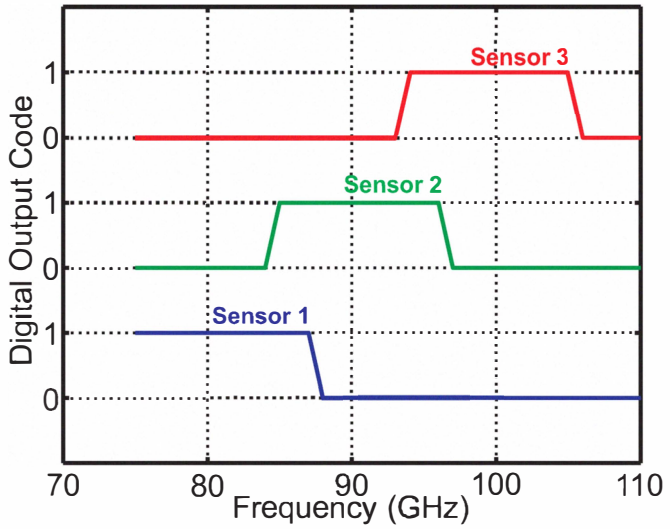

Fig. 8. Measured digital outputs of the proposed DiPAD configured as a frequency demodulator for frequencies from 75 to 110 GHz (W-band). Input power 3dBm.

To test the phase demodulation performance of the DiPAD, both ends were fed with a 110 GHz CW carrier originating from the same mm-wave source as shown in Fig.7b. A W-band differential phase shifter was employed to sweep the relative phase of the two inputs while the output from each of the three sensors was recorded. As shown in Fig.9, each sensor responds with a "1" for a small range of phase differences. Sensor 2 is reasonably centered at 180 degrees while sensor 1 and sensor 3 are centered around 90 and -90 degrees. A small region is also available at 0 degrees where all 3 sensors are zero. With these 4 regions (010 100 001 000) it is possible to implement a QPSK demodulator by mapping these four codes into two bit output codes (00 01 10 11) with simple combinational logic circuits. Note that because sensors 1 and 3 are not placed at the end of the DiPAD the voltage standing-wave nulls occurring at both ends of the transmission line are not sensed. The measured "000" case at 0 degrees corresponds to the same 0 degree case in Fig.5.

VIII. Conclusions

Measurements of the proposed DiPAD demodulator demonstrate that it is capable of directly demodulating both frequency and phase modulated mm-wave carriers into digital signals. The DiPAD demodulator eliminates the mixer and analog-to-digital converter of the receiver enabling extremely low power and compact designs. The performance of the proposed DiPAD demodulator is summarized in table I.

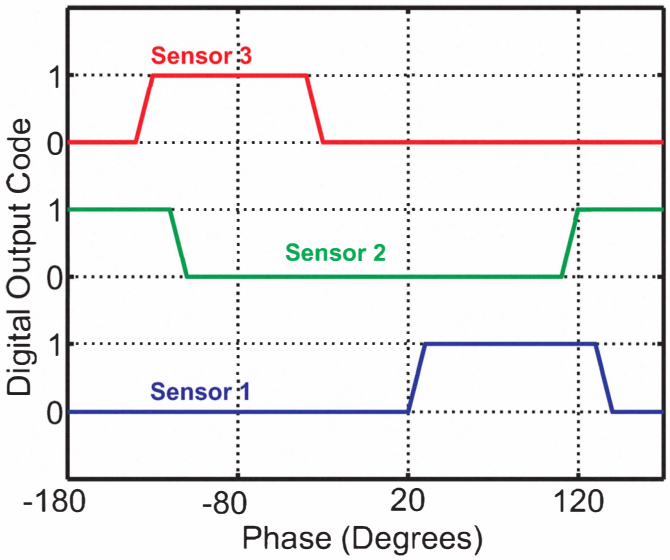

Fig. 9. Measured digital output response of the proposed DiPAD at 110 GHz as the phase between two inputs are swept from 0 to 360 degrees. Input tone power 3dBm per tone.

TABLE I
Performance of proposed DiPAD demodulator.

Technology	65nm CMOS
Carrier Frequency	75-110 GHz
Required Input Power	3 dBm
Power Consumption	0.47mW
Die Area	0.16mm^2

IX. Acknowledgments

The authors are grateful to tsmc for their excellent CMOS 65nm foundry support. The authors would also like to thank Zhiwei Xu, Qun Gu, and Y.C. Wu for several helpful technical discussions.

References

[1] T. LaRocca, S. Tam, D. Huang, Q. Gu, W. Hant, and M. F. Chang, "Millimeter-Wave CMOS Digital Controlled Artificial Dielectric Differential Mode Transmission Lines for Reconfigurable ICs," *IEEE MTT-S IMS*, pp. 181-184, 2008

[2] T. LaRocca, J. Liu, F. Wang, F. Chang, "Embedded DiCAD linear phase shifter for 57-65GHz reconfigurable direct frequency modulation in 90nm CMOS," *IEEE RFIC*, pp.219-222, 2009

[3] W.E. Kock, Metallic Delay Lenses, *Bell Syst. Tech. J.*, vol. 27, pp.58-82, 1948.

[4] R.E. Collin, Field Theory of Guided Waves 2nd Edition, New Jersey: IEEE Press, 1991.

978-1-61284-757-3/11/$26.00 C2011 IEEE